

THE EFFECT OF SQUEEZE CASTING PROCESS ON THE MICROSTRUCTURE, MECHANICAL PROPERTIES AND WEAR PROPERTIES OF HYPEREUTECTIC Al–Si–Cu–Mg ALLOY

Jianfei Hao, Huixin Luo, Jiancong Bian, Yuanji Shi, and Baoyi Yu

School of Material Science and Engineering, Shenyang University of Technology, Shenyang 110870, China

Runxia. Li 

School of Material Science and Engineering, Dongguan University of Technology, Dongguan 523808, China

Copyright © 2021 American Foundry Society
<https://doi.org/10.1007/s40962-021-00575-x>

Abstract

The effects of the squeeze casting process on the microstructure, mechanical properties and wear characteristics of hypereutectic Al–Si–Cu–Mg alloys have been investigated by optical, scanning and transmission electron microscopy and mechanical property test; the wear behaviour was investigated using a pin-on-disc configuration; alloy ingots were prepared by gravity casting, liquid squeeze casting and semisolid squeeze casting. The results show that the Si phase was refined and the α -Al dendrites transformed to rosette grains after semisolid squeeze casting. The peak intensity of the second phase decreased after extrusion, indicating that extrusion promotes the dissolution of solute elements into the matrix. Among the three casting processes, the alloys formed by semisolid

squeeze casting had the best mechanical properties. Tensile strength, elongation and Brinell hardness reached 187.67 MPa, 2.33% and 142.5 HB, respectively. After semisolid squeeze casting, the morphology of the wear surface was flat and the number of spalling pits and furrows is less. Meanwhile, the friction coefficient and wear loss of the alloy sample are minima. Due to the uniform distribution of Si phases and equiaxed crystallization of α -Al phase in semisolid squeeze casting Al–Si–Cu–Mg alloys, the wear resistance is markedly enhanced.

Keywords: *squeeze casting process, Al–Si–Cu–Mg alloys, microstructure, mechanical properties, wear properties*

Introduction

Hypereutectic Al–Si alloy has the advantages of low specific gravity, good wear and corrosion resistances, low coefficient of linear expansion and excellent casting performance. It is widely used to prepare automobile engines and some complex shape parts.^{1–5} Adding appropriate amounts of Cu and Mg into Al–Si alloys can form a variety of second phases that can strengthen the matrix and improve the strength of the alloy. As the hypereutectic Al–Si alloys contain massive primary Si and lath eutectic Si phases, it has a great cleavage effect on the alloy matrix and seriously affects the mechanical properties of the alloy. Although the morphology of the Si phase can be improved by heat treatment in the later stage, the improvement in

mechanical properties is limited. In the early stage of the experiment, the morphology and size of the Si phase in the alloy are obviously affected by adjusting the forming process. After the later heat treatment process, the mechanical properties of the alloy will be greatly improved.

Squeeze casting is a generic term to specify a fabrication technology where the solidification process is promoted under high pressure, which combines advantages of die casting and die forging into a single operation where molten metal is solidified under applied hydrostatic pressure. It not only has the advantages of a simple casting process, low production cost and complex part shapes, but the products also have the characteristics of fine grains, uniform structure, good mechanical properties and high forming precision.^{6–9} The effects of squeeze casting parameters on the microstructure and mechanical

properties of aluminium alloys and magnesium alloy and their composites have been investigated extensively. Lus¹⁰ studied the effect of casting parameters on the microstructure and mechanical properties of squeeze cast A380 aluminium die-cast alloy. The results show that when the pressure increases from 10 to 50 MPa, the dendrite spacing decreases to 5.7 μm and the strength and elongation reach 236 MPa and 2.5%, respectively. Maleki et al.¹¹ studied effects of squeeze casting parameters on the microstructure of LM13 alloy. The results show that applying pressure during solidification decreases the grain size and SDAS of the primary phase and modifies the eutectic silicon particles. Lin et al.¹² studied the effects of high-pressure rheo-squeeze casting on Fe-containing intermetallic compounds and mechanical properties of Al-17Si-2Fe-(0, 0.8) V alloys. The result shows that the coarse FIMCs are fractured and the sizes of the block-like δ phase and short needle-like β phase are decreased as the pressure is increased. Dao et al.¹³ studied the effects of process parameters on microstructure and mechanical properties in AlSi9Mg connecting-rod fabricated by semisolid squeeze casting. The results show that the non-dendritic primary α -Al particles distribute uniformly throughout the connecting-rods. With increased applied squeeze pressure, the size of α -Al particles decreases while the shape factor and the mechanical properties of the connecting-rods increase. Alireza Hekmat-Ardakan¹⁴ and Lasa¹⁵ et al. studied wear behaviour of hypereutectic Al-Si-Cu-Mg casting alloys. The results show that the wear resistance of the alloy is better when the content of primary Si and Mg is high. Pratheesh et al.¹⁶ studied the effects of the squeeze pressure on the microstructure, wear characteristics and mechanical properties of near-eutectic Al-Si piston alloys. The results show that the squeeze-cast samples have better mechanical properties and tribological properties. Most scholars have only studied the influence of a forming process or process parameters on the microstructure and mechanical properties of the alloys. However, little research has been conducted on the mechanism of improving the properties of the alloy and the reasons for the difference of microstructure and properties between liquid squeeze casting and semisolid squeeze casting.

In this paper, the macrostructure, Si phase morphology, dislocation density, mechanical properties and friction and wear properties of Al-Si-Cu-Mg alloys under different casting processes were studied. The hypereutectic Al-Si-Cu-Mg alloys were prepared by different casting process. The optimal casting process of Al-Si-Cu-Mg alloys was determined within the experimental range. The differences in microstructure and mechanical properties of the alloy under different casting processes were analysed.

Materials and Experimental Procedures

Al-Si-Cu-Mg alloy was prepared by melting pure aluminium ingot (99.7%, mass percentage), pure magnesium ingot (99.8%) and Al-20Si (wt%) and Al-50Cu (wt%) alloy. The chemical composition of the alloy was determined using a SPECTROMAX photoelectric direct reading spectrometer. The chemical composition of the alloy is summarized in Table 1.

During the melting process, the pure aluminium ingot and Al-Si master alloy were put into the melting furnace first and the melting furnace was heated to 760 °C. When the alloy in the furnace was completely melted, Al-50Cu (wt%) alloy and pure Mg ingots were added. After the alloy ingot was completely melted, C_2Cl_6 was used to refine and degas the molten alloy. Al-5Ti-B was used to refine the grains and Si phase was modified by Al-10Sr master alloy. The addition of Al-5Ti-B alloy into Al melt will form fine dispersed Al_3Ti and B_2Ti solid particles, which can be used as the nucleation core of Al matrix, increase the reaction interface and the number of nuclei, reduce the number of crystals and play the role of grain refinement. In this experiment, gravity casting, liquid squeeze casting and semisolid squeeze casting were selected. The specific process is shown in Figure 1. Gravity casting was formed by natural solidification in the metal die after refining and standing. Liquid squeeze casting was to pour the liquid metal in the die and squeeze under 600 MPa. The pouring temperature of molten metal was 720 °C. The 5000 KN vertical extruder is shown in Figure 2a. The extrusion process parameters are shown in Table 2. The semisolid squeeze casting was to pour the semisolid slurry into the die and squeeze forming. Semisolid slurry was prepared by electromagnetic stirring. The model of electromagnetic agitator is TSOJ3-G as shown in Figure 2b and c. First, the molten liquid was poured into another die in the electromagnetic agitator, the preheating temperature of the die was 600 °C to prevent the slurry from solidifying too fast. Then, the electromagnetic agitator was rebooted. The input frequency was 6 HZ and the input current was 80 A. The stirring time was kept at 10–12 s. Finally, the semisolid slurry was rapidly poured into the die for extrusion forming. The pouring temperature of semisolid slurry was 600 °C. The specific pressure was 600 MPa.

The samples were cut at the half radius of the cross section of the alloy ingots. The size and sampling position of the extruded specimen are shown in Figure 3a. The ingot is in

Table 1. Chemical Composition of the Alloy (wt%)

Alloys	Si	Cu	Mg	Fe	Al
	17.75	4.36	0.47	0.08	Bal.

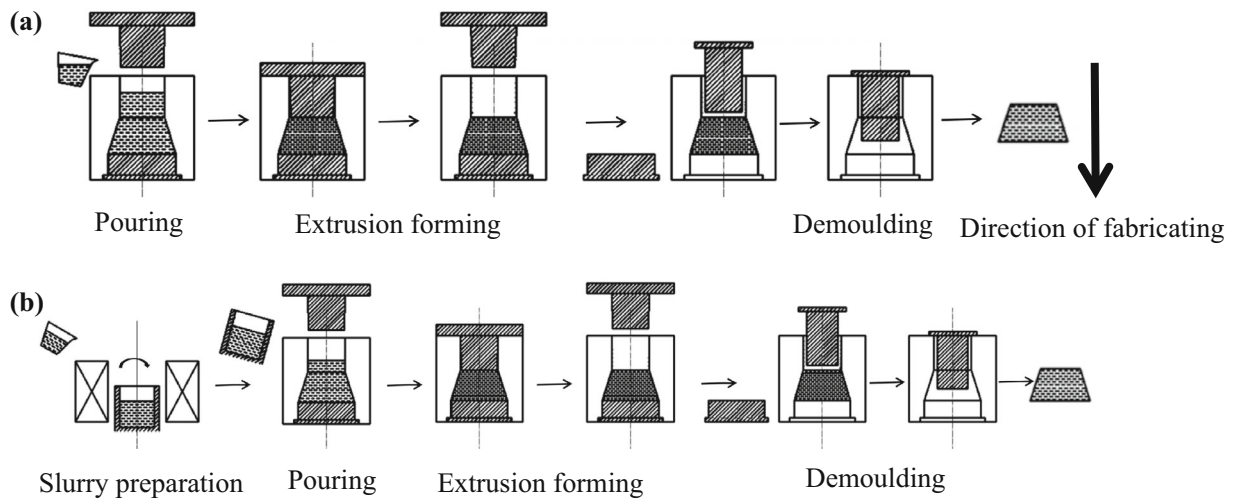


Figure 1. Schematic diagram of forming process. (a) Liquid squeeze casting; (b) Semisolid squeeze casting.

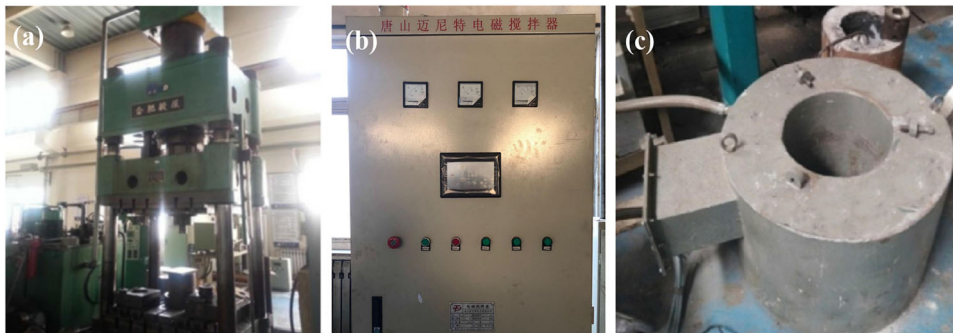


Figure 2. Forming equipment. (a) Vertical extruder; (b) Control cabinet; (c) Electro-magnetic agitator.

Table 2. Parameters of Extrusion Casting Experiment

Extrusion speed/mm s ⁻¹	Die temperature/°C	Holding time/s	Die coating
5±2	380±5	60±5	Graphite oil

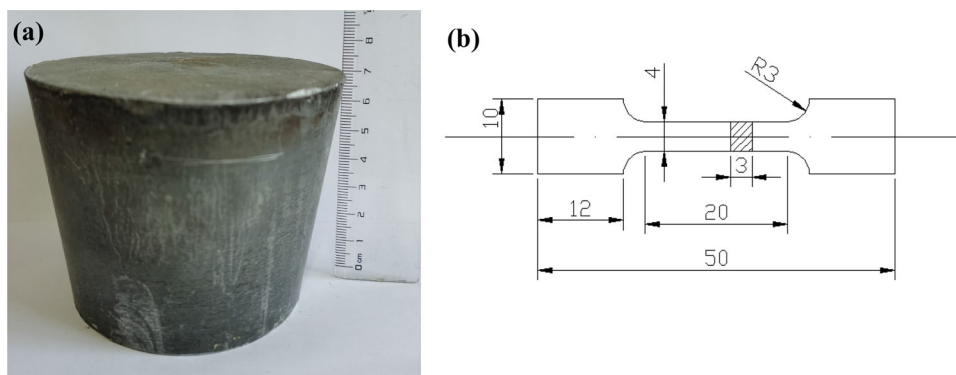


Figure 3. Specimen diagram. (a) Extruded specimen; (b) Tensile specimen size.

the shape of a circular truncated cone with a height of 700 ± 5 mm. After grinding, polishing and corrosion, the macrostructure was observed using a LEICA-DMI3000M metallographic microscope and the microstructure was observed using a JMS-6301F cold field scanning electron microscope. The composition analysis of the intermetallic compounds was performed by energy-dispersive X-ray spectroscopy. X-ray diffraction analysis was carried out using an XRD-7000 X-ray diffractometer with Cu-K α in the 20–80° scanning range and a 2°/min scanning speed. The mechanical properties were tested on a WGW-100H universal testing machine. The loading rate was 1 mm/min. The loading type was load-controlled. The standard for tensile testing is according to GB 228-2000. The tensile specimen size is shown in Figure 3b. Friction and wear test of the hypereutectic Al–Si–Cu–Mg alloys was investigated on an MMU-5G pin-on-disk friction wear tester with a 70 N load, 30 min wear time and 200 r/min speed. The form of wear was pin disc wear, and the wear mode was dry friction wear. The test standard for friction and wear specimens is GB 12444.1-1990. The wear test samples with dimensions of $\Phi 4$ mm \times 15 mm were cleaned by acetone solution before and after wear tests. The hardness was tested by forcing a tungsten carbide ball with a 2.5 mm diameter onto the polished surface of the samples with an applied load of 62.5 N for 30 s. Five data points were collected and an average was taken for each Brinell hardness value. The standard for hardness testing is according to GB / T 231.1-2009.

Results and Discussion

Microstructure of Al–Si–Cu–Mg Alloys

Figure 4 shows the microstructure from the optical microscope (OM) and scanning electron microscope (SEM) images of the hypereutectic Al–Si–Cu–Mg alloys under gravity casting. It can be seen from Figure 4a that the hypereutectic Al–Si–Cu–Mg alloys contain massive primary Si phase particles, lath eutectic Si phase and α -Al

dendrite. It can be seen from Figure 4b that there are white short rod-like second phase and grey fish-net second phase. Figure 5 shows the EDS spectrum of the hypereutectic Al–Si–Cu–Mg alloys. According to EDS analysis, the white short rod second phase is θ (Al_2Cu) phase, and the grey fish-net second phase is Q ($\text{Al}_5\text{Cu}_2\text{Mg}_8\text{Si}_6$) quaternary phase.

Effect of Casting Process on Microstructure

Figure 6 shows the microstructure of Al–Si–Cu–Mg alloys under different casting conditions. As can be seen from the figure, the forming process has a great influence on the microstructure of the alloys. Figure 6a shows the microstructure of hypereutectic Al–Si–Cu–Mg alloys under gravity casting. There are large primary Si phase, lath eutectic Si phase and α -Al dendrite. Figure 6b shows the microstructure of hypereutectic Al–Si–Cu–Mg alloys under liquid squeeze casting. Compared with gravity casting, the size of primary Si in the alloy is reduced, the eutectic Si phase distribution is more uniform and the change of α -Al dendrite is not obvious. Figure 6c shows the microstructure of hypereutectic Al–Si–Cu–Mg alloys under semisolid squeeze casting. The primary Si phase in the alloy structure becomes finer and rounder, the eutectic Si phase is smaller and evenly distributed, and most α -Al dendrites are transformed into approximated to equiaxed crystals. Table 3 shows the primary Si size, SDAS and the morphology of α -Al dendrite of the hypereutectic Al–Si–Cu–Mg alloy under the three processes. After semisolid extrusion, the average size of the primary Si in the structure is 22.1 ± 0.7 μm , and the SDAS is 3.5 ± 0.7 μm .

The refinement and non-dendriticization of the alloy structure can be attributed to the increased crystalline core in the melt and the elimination of dendrite growth conditions. When the liquid metal solidifies under pressure, the gap between the metal and mould will be significantly reduced and the heat conductivity coefficient increases, which will lead to accelerating the solidification rate of the

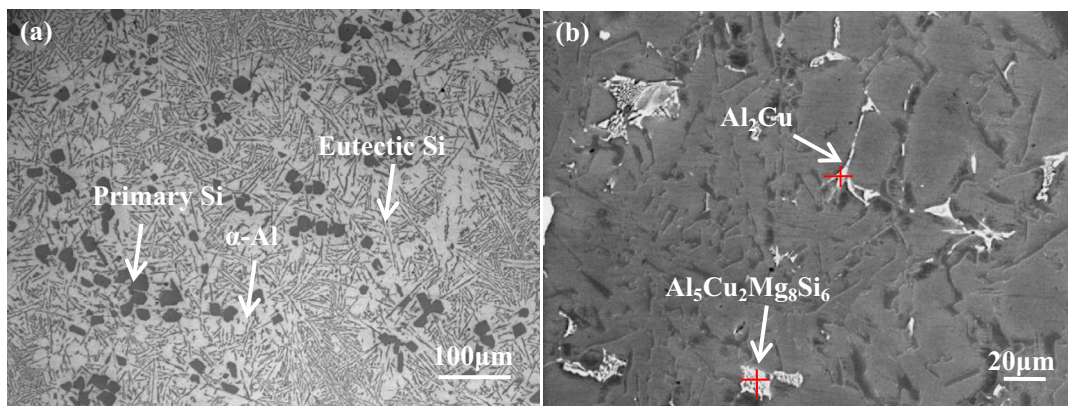


Figure 4. Microstructure of Al–Si–Cu–Mg alloys under gravity casting.

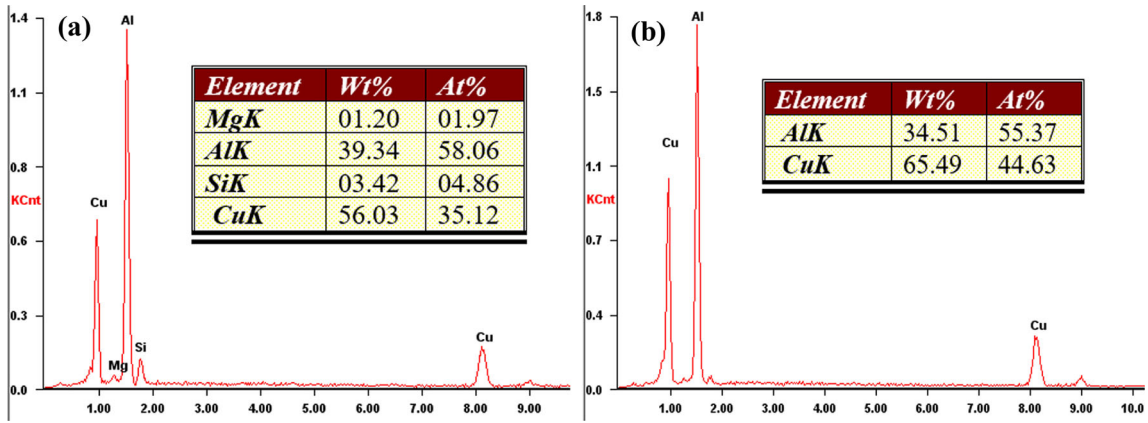


Figure 5. EDS spectrum of hypereutectic Al-Si-Cu-Mg alloys.

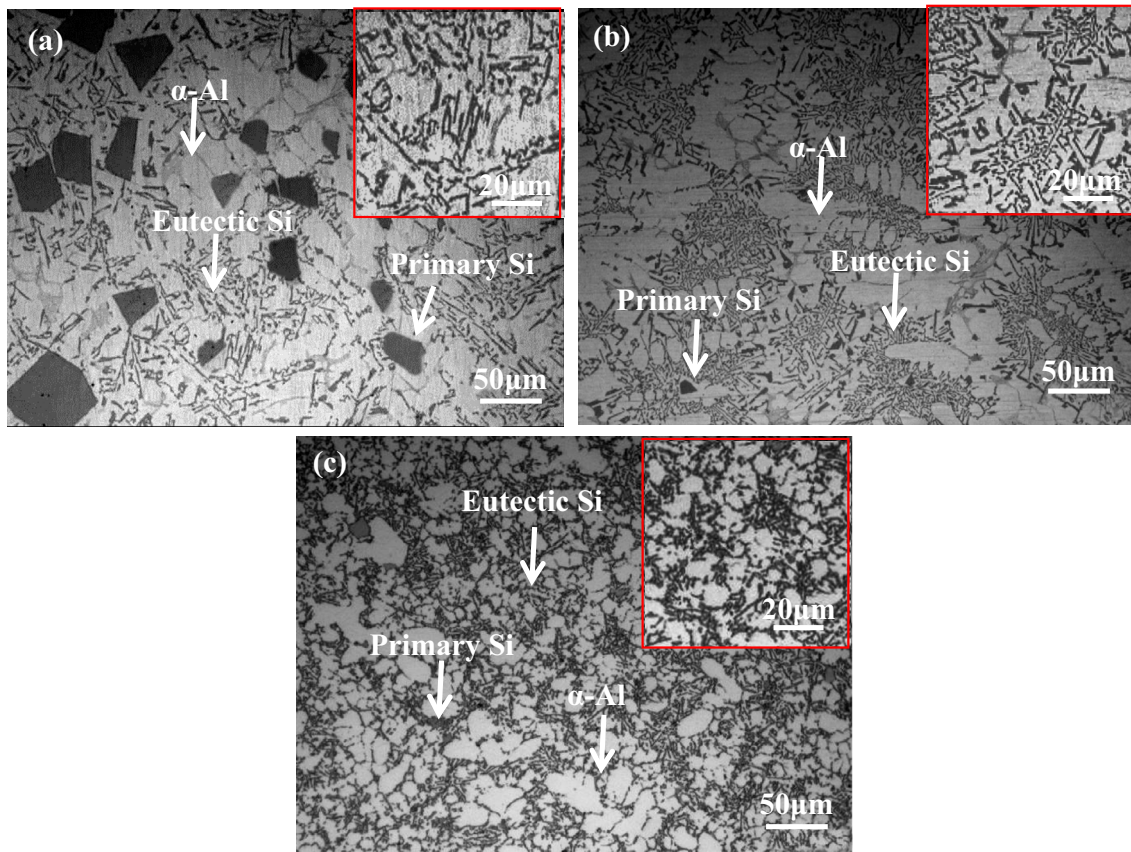


Figure 6. Microstructure of Al-Si-Cu-Mg alloys under different casting processes. (a) Gravity casting; (b) Liquid squeeze casting; (c) Semisolid squeeze casting.

alloy. The nucleation rate of the alloy during solidification can be expressed by the following Eqn. (1):^{10,11}

$$I = \exp\left[\left(\frac{-\alpha\gamma^3 V_s}{RT_m H_m^2}\right)\tau^2(1-\tau)^{-1}\right] \exp\left[\frac{-\Delta G}{RT_m}(1-\tau)^{-1}\right]$$

Eqn. 1

where α is a geometric constant, γ is interfacial tension (N/m), V_s is the solid atomic volume (m^3), H_m is the latent heat of solidification (J/mol), T_m is melting temperature

(K), ΔG is the activation energy of nucleation (J/mol), and R is the gas constant (8.31 J/mol·K).

Eqn. (2) is obtained by comparing $I(P)$ and $I(P_0)$, the respective nucleation rates under pressure P and P_0 :^{12,13}

$$\frac{I(P)}{I(P_0)} = \exp[\gamma^3(P_0) - \gamma^3(P)] \exp\left[\frac{\Delta G(P_0) - \Delta G(P)}{RT}\right]$$

Eqn. 2

Pressure can reduce the activation energy of nucleation.

Table 3. Characteristics of Microstructure of Al–Si–Cu–Mg Alloys

	Si particle size/ μm	SDAS/ μm	Morphology of $\alpha\text{-Al}$
Gravity casting	48.7 \pm 1.2	6.4 \pm 0.7	Dendritic
Liquid squeeze casting	28.6 \pm 1.9	5.2 \pm 0.6	Dendritic
Semisolid squeeze casting	22.1 \pm 0.7	3.5 \pm 0.7	Rosette

$\Delta G(P_0) > \Delta G(P)$, so $I(P) > I(P_0)$. This behaviour indicates that pressure can increase the nucleation rate during solidification, so the microstructure of the solidified alloy under pressure is refined.

The microstructure refinement after semisolid squeeze casting is due to the slurry prepared by an electromagnetic stirring process; an electromagnetic stirring process can increase the nucleation core and the number of free crystal grains from the crystallizer wall. Through the repeated stretching and compression of electromagnetic oscillation force, the wetting of a melt to high-temperature solid compounds and quasi solid-phase atomic clusters is increased and the critical free energy of heterogeneous nucleation is reduced. Under a high degree of supercooling, a large number of crystal nuclei are attached to the melt, resulting in heterogeneous nucleation, which refines the grains. Due to the simultaneous existence of high-pressure solidification and plastic deformation, the metal will crystallize and solidify under pressure and the shrinkage cavity and porosity formed by solidification shrinkage are eliminated. Therefore, castings with dense structure and no porosity, shrinkage or other defects can be obtained.

The as-cast XRD patterns of Al–Si–Cu–Mg alloys are shown in Figure 7. Analysing the XRD curves further shows that there are Q ($\text{Al}_5\text{Cu}_2\text{Mg}_8\text{Si}_6$) and θ (Al_2Cu) phases besides Si and $\alpha\text{-Al}$ dendrites in the matrix. The

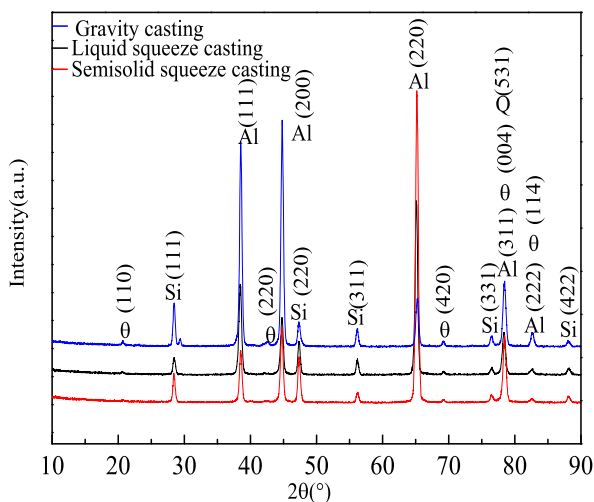


Figure 7. XRD patterns of Al–Si–Cu–Mg alloys under different casting processes.

positions of diffraction peaks are the same under different casting processes but the peak intensity corresponding to the θ (Al_2Cu) phase and the Q ($\text{Al}_5\text{Cu}_2\text{Mg}_8\text{Si}_6$) phase under the squeeze casting process is lower than that formed by metal mould gravity casting, which indicates that the squeeze casting process can promote the solute elements moving into the alloy matrix and play a role of solution strengthening.

Effect of Casting Process on Dislocation Density

Figure 8 shows the dislocation structure of Al–Si–Cu–Mg alloys under different casting processes. Figure 9 shows the quantitative calculation of the dislocation densities of four different crystal planes. It can be seen from the figure that the forming process has a great influence on the dislocation of the alloy. Figure 8a shows the dislocation structure of the alloy under gravity casting and there are a small number of dislocation lines in the alloy structure. It can also be seen from the calculation results that the dislocation density of the alloy under gravity casting is low. Figure 8b shows the dislocation structure of the alloy under liquid squeeze casting. Compared with gravity casting, the number of dislocation lines in the alloy is significantly increased. From the calculation results in Figure 9, the dislocation density of the different crystal planes of the alloy under liquid squeeze casting is also higher than that of gravity casting. Figure 8c is the dislocation structure of the alloy under semisolid squeeze casting. There are more dislocation lines in the alloy structure. The quantitative calculation shows that the dislocation density of the alloy structure after semisolid squeeze casting is higher than that of the liquid extrusion sample.

In the process of extrusion solidification under high pressure, the effect of pressure on the diffusion coefficient of solute can be expressed using Eqn. (3):^{17–20}

$$D = RT\delta^{-1}\eta_0 e^{-\frac{pV_0}{RT}} \quad \text{Eqn. 3}$$

where δ is the atomic free path length (m), η_0 is the atmospheric viscosity at the same temperature (Pa·s) and V_0 is the atmospheric volume at the same temperature (m^3/mol).

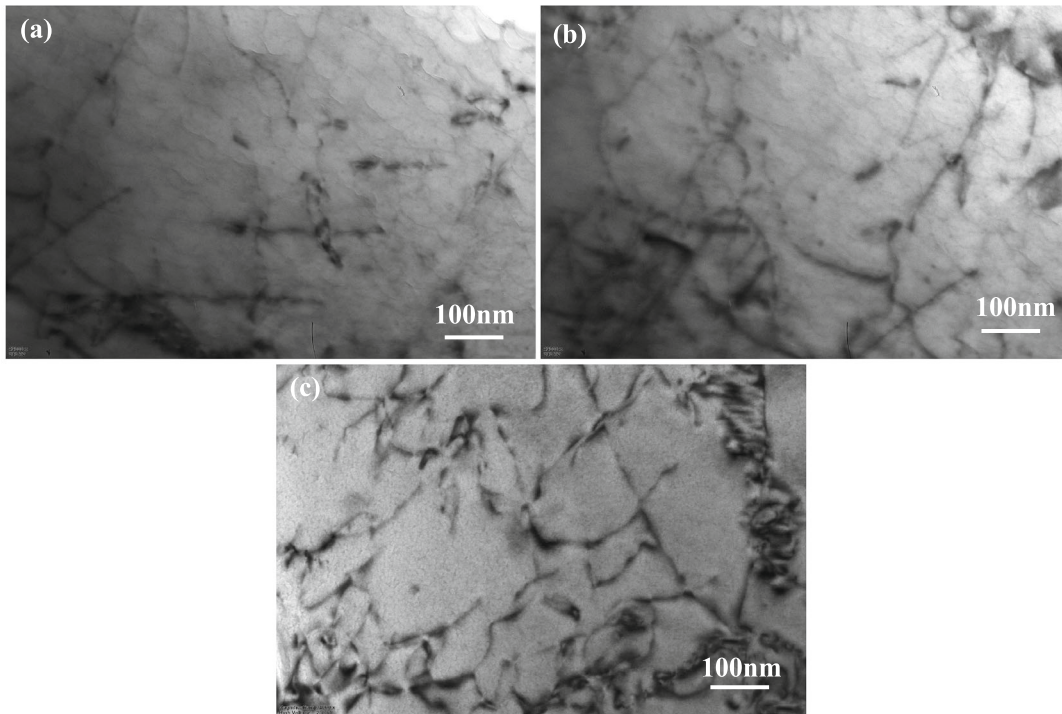


Figure 8. Dislocation structure of Al-Si-Cu-Mg alloys under different casting processes (a) Gravity casting; (b) Liquid squeeze casting; (c) Semisolid squeeze casting.

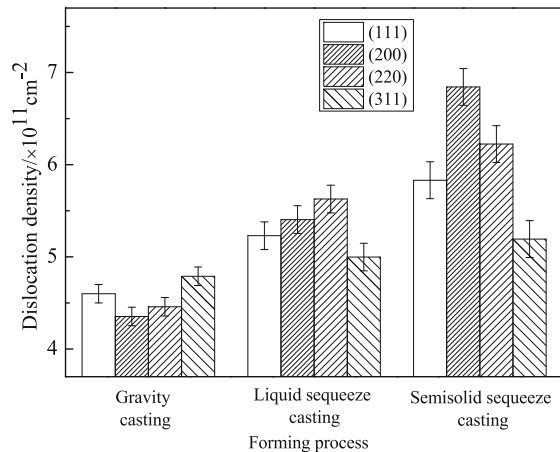


Figure 9. Dislocation density of Al-Si-Cu-Mg alloys under different casting processes.

It can be seen from Eqn. (3) that with the increase in pressure, the diffusion speed of solute atoms in liquid metal slows down, Si atoms form a supersaturated solid solution in the matrix, and plastic deformation will occur during the extrusion process, which increases the possibility of lattice vacancy and dislocation aggregation. In the alloy structure, the relationship between the relative density of dislocation N and the element concentration C in the alloy can be expressed using Eqn. (4):²¹⁻²³

$$N = B^2 \sqrt{C} \quad \text{Eqn. 4}$$

where B is the integral constant, which is measured experimentally.

In the semisolid squeeze casting process, since the slurry is semisolid, a large plastic deformation will occur during the extrusion process. At this time, the internal energy of the alloy is high and there are large vacancy defects, which promote the solid solution of Si into the matrix. With the increase of Si atom concentration in the alloy structure, the dislocation density increases.

Effect of Casting Process on Mechanical Properties

Figure 10 shows the mechanical properties of hypereutectic Al-Si-Cu-Mg alloys under different casting processes. Among the three casting processes, the Al-Si-Cu-Mg alloys formed by a semisolid squeeze casting process have the best mechanical properties. Tensile strength, elongation and Brinell hardness reach 187.67 MPa, 2.33% and 142.5 HB, respectively. Compared with gravity casting, they are increased by 55.07%, 56.38% and 29.66%, respectively. Table 4 shows the strength of Al-Si alloys with different compositions under different forming processes. Compared with other experimental results, the experimental results obtained in this paper have better comprehensive mechanical properties. The tensile strength of as-cast Al-20Si alloy can reach 199 MPa, but the elongation is only 0.58%. The strength and elongation of as-

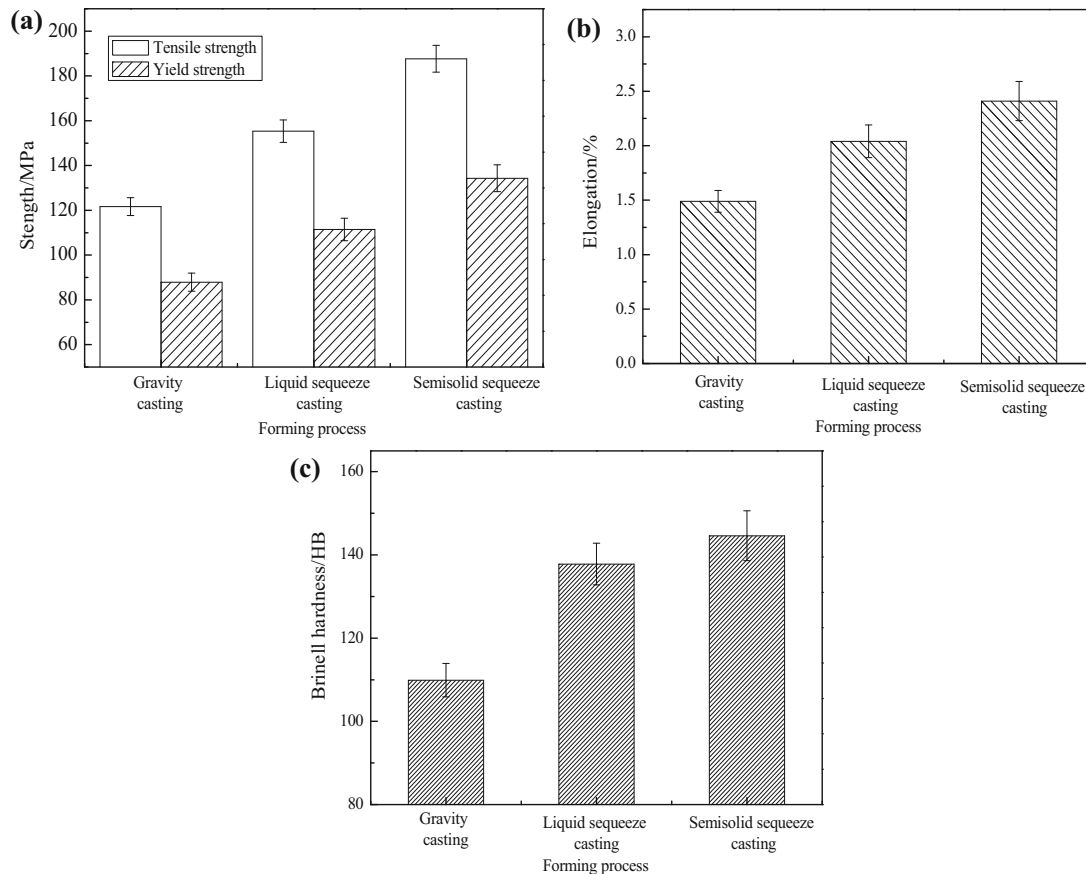


Figure 10. Mechanical properties of Al-Si-Cu-Mg alloys under different forming processes.

cast hypoeutectic Al-Si alloy are also slightly lower than those of the experimental alloy. After comparison, the alloy in this paper exhibits both excellent hardness elongation and relatively high strength after semi-extrusion.

In the process of liquid squeeze casting, with the increase in pressure, the growth rate of crystal will be accelerated, and the growth of crystal will be restrained by the growth of adjacent nuclei, which will hinder the growth trend and refine the structure. Meanwhile, due to the extrusion force during the solidification of the alloy, the primary α -Al dendrites will be broken in the initial stage of solidification, which will cause dendrites fragmentation.^{28,29} In the semisolid squeeze casting, the semisolid slurry prepared by the electromagnetic stirring process has a more uniform structure distribution. When the slurry temperature is 600 °C, the cooling rate is faster and the melt is in a state of greater undercooling. A large number of free nuclei have been formed in the melt. Coupled with the chilling effect in contact with the mould, the number of nucleation increases and the nucleation rate accelerates. The nucleated nuclei are extruded and solidified before they can continue to grow, and finally the uniform and fine primary Si phase is formed.^{30,31} The variation of the mechanical properties is closely associated with the microstructural characteristics in the alloys, because the size of the Si phase is smaller and

the distribution of Si phase is more uniform after semisolid squeeze casting. The equiaxed α -Al dendrite makes the anisotropy small and the deformation is even during processing. Meanwhile, more solute elements are dissolved in the structure to strengthen the matrix. The structure contains more dislocation lines, which will also increase the strength of the alloy, because the size of the Si phase is smaller and the distribution of Si phase is more uniform after semisolid squeeze casting. The equiaxed α -Al dendrite makes the anisotropy small and the deformation is even during processing. Meanwhile, more solute elements are dissolved in the structure to strengthen the matrix. The structure contains more dislocation lines, which will also increase the strength of the alloy. Therefore, the alloy has higher mechanical properties after semisolid extrusion.

Figure 11 is the fracture morphology of Al-Si-Cu-Mg alloys under different casting processes. In Figure 11a, there are a large number of cleavage surfaces and a large number of micro-cracks, the size of micro-cracks is about 30 μm in the fracture surface of the alloy under gravity casting, which easily causes brittle fracture of the alloy. The primary Si phase is a brittle phase that is not easily deformed; when it is loaded, the coarse bulk primary Si phase is prone to stress concentration. When the stress intensity reaches the limit, the primary Si phase will break.

Table 4. Comparison of Mechanical Properties of Al-Si Alloys

Materials	State	UTS (MPa)	Elongation (%)	Hardness	References
Al-17.75Si-4.36Cu-0.47Mg	As-Cast	187.67	2.33	142.5 HB	Present work
Al-17Si-2Cu-0.4Mg	As-Cast	175	0.35	–	12
Al-12.35Si-3.04Cu-1.03Mg	As-Cast	135	–	95 HB	16
Al-8.54Si-2.34Cu-0.23Mg	As-Cast	160.11	1.47	–	24
Al-9.75Si-1.44Cu	As-Cast	182	0.8	94 HB	25
Al-20Si	As-Cast	199	0.58	89 HV	26
Al-10.9Si-2Cu-0.1Mg	As-Cast	187.1	2.9	73.9 HB	27

In Figure 11b, compared with gravity casting, the number of large-scale cleavage plane is reduced, and more small-scale quasi-cleavage planes are added. Meanwhile, the number of micro-cracks is significantly reduced, and the size is reduced to about 10 μm . After liquid squeeze casting, the size of the primary Si phase in the alloy matrix decreases and the distribution is more uniform, which reduces the risk of crack aggregation and fracture. Figure 11c shows the fracture morphology of the alloy formed by semisolid squeeze casting. There are more small-scale quasi-cleavage planes and tear ridges in the tensile fracture surface of the alloy and the number and size of cleavage platforms are significantly reduced. The size of micro-cracks is about 5 μm . So, the mechanical properties of the alloy are greatly improved. Compared with liquid squeeze casting, the semisolid squeeze casting process uses electromagnetic stirring technology to prepare the slurry, which plays a key role in refining the alloy structure while improving the morphology of the primary Si phase and reducing its cleavage effect on the substrate.

Effect of Casting Process on Wear-Resisting Properties

Figure 12 shows the variation curves of the friction coefficient and wear loss of Al-Si-Cu-Mg alloys under different casting processes. The average friction coefficients of the alloy are 0.3878, 0.3658 and 0.3512 for gravity, liquid squeeze and semisolid squeeze casting, respectively. Under a semisolid squeeze casting process, the friction coefficient fluctuation curve of Al-Si-Cu-Mg alloys is more stable. The wear losses (m) for the casting processes are 14.6, 10.8 and 8.4 mg, respectively. Under the condition of dry friction, the relationship between wear loss and hardness of an alloy sample can be expressed as follows: ^{32,33}

$$m = kvt \frac{W}{H} \quad \text{Eqn. 5}$$

where m is the wear loss (mg), v is the friction sliding speed (mm/s), t is the friction time (s), W is the

positive load (N) and H is the hardness of the alloy (HB).

According to Eqn. (5), the wear loss of the alloy is proportional to the ratio of load to hardness. With increased Brinell hardness, the wear loss of the alloy decreases gradually.

Figure 13 shows the wear surface morphology of hypereutectic Al-Si-Cu-Mg alloys under different casting processes. There are irregular chipping pits and strip furrows of different depths on the surface morphology formed by gravity casting alloy samples. After liquid squeeze casting, the size of the chipping pits on the wear surface is reduced, the shape is still irregular and the depth of the furrow becomes shallower. After semisolid squeeze casting, the morphology of the wear surface is relatively flat and the number of spalling pits and furrows is less. Meanwhile, the friction coefficient and wear loss of the alloy sample are minima and the wear resistance of the alloy is the best. After semisolid squeeze casting, the Si phase size in the alloy is smaller, the eutectic Si distribution is more uniform and the α -Al dendrites are also transformed into equiaxed crystals.³⁴ Therefore, during the friction process, the furrow of the wear surface is shallow.

Conclusion

In this work, the effects of the casting process on the microstructure, mechanical properties and wear properties of Al-Si-Cu-Mg alloys were investigated. Based on the experimental data and simulation results, the following conclusions can be drawn:

After semisolid squeeze casting, the Si phase is refined and the α -Al dendrites change to equiaxed. The peak intensity of the second phase decreases, indicating that extrusion promotes the solid solution of solute elements into the matrix. The dislocation density in the alloy matrix is higher than that in the other two casting processes.

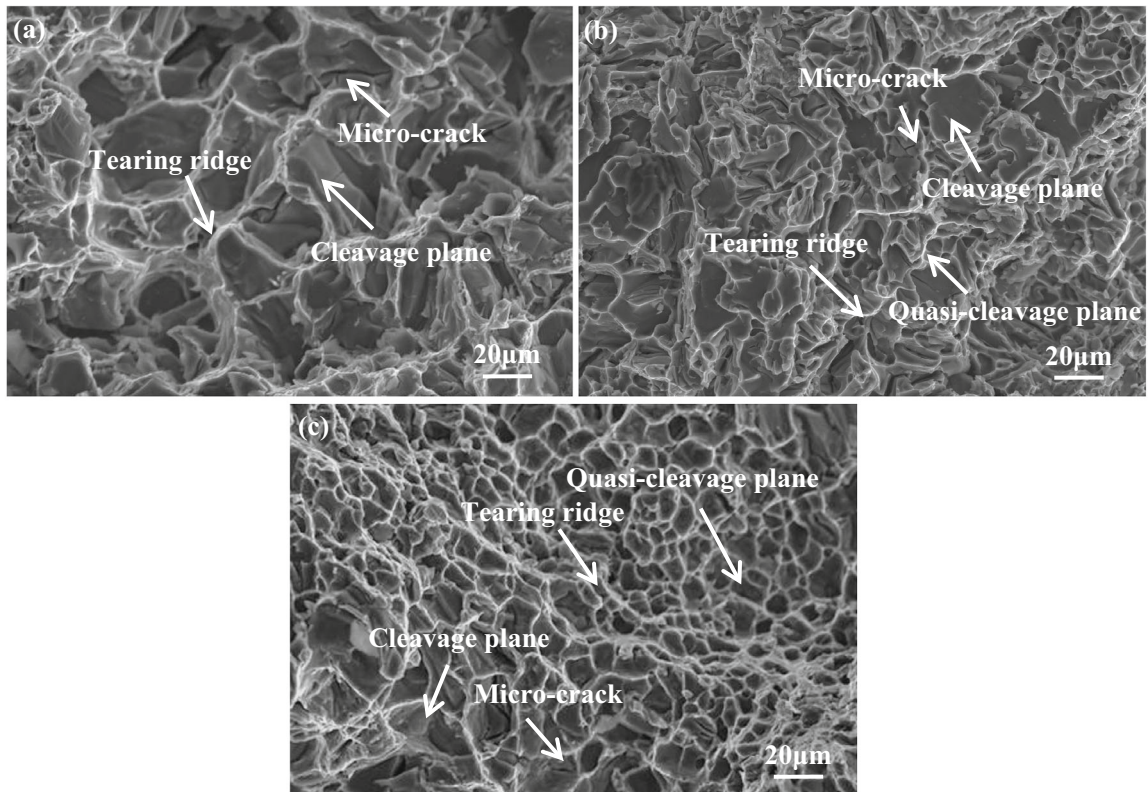


Figure 11. Fracture morphology of Al-Si-Cu-Mg alloys under different casting processes.

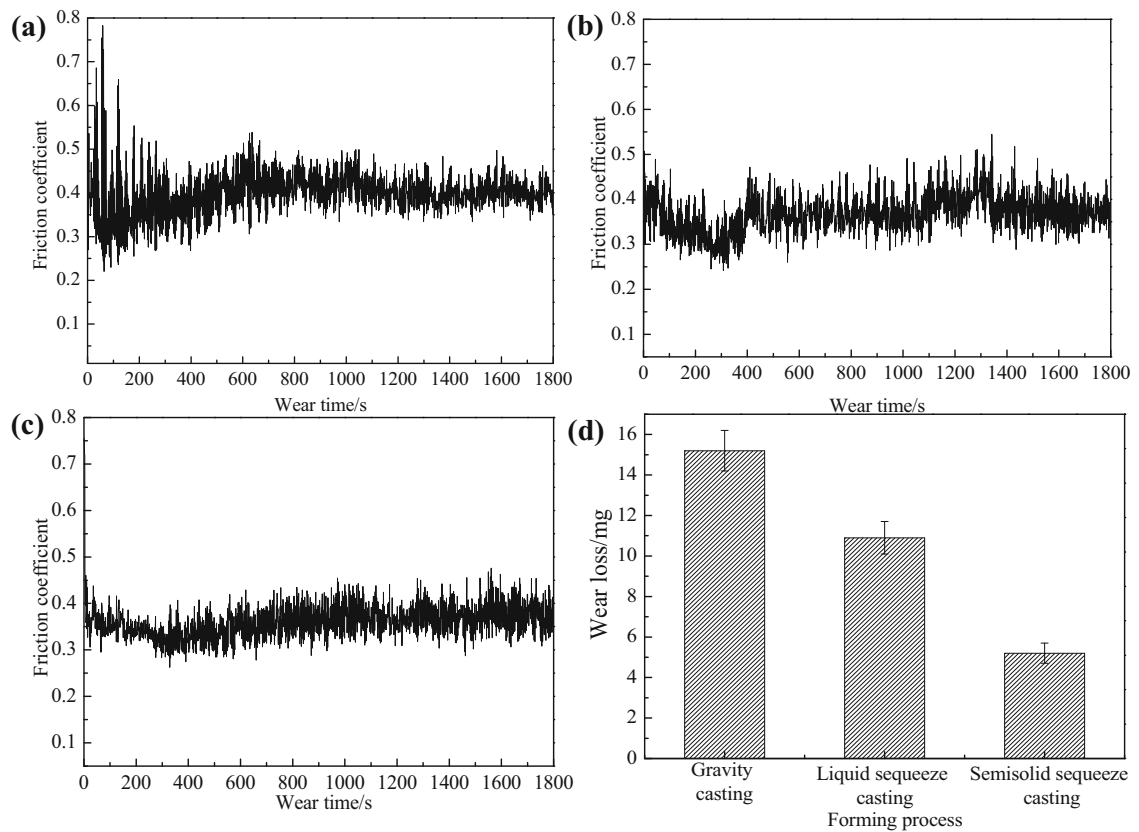


Figure 12. Friction coefficient and wear loss of Al-Si-Cu-Mg alloys under different casting processes.

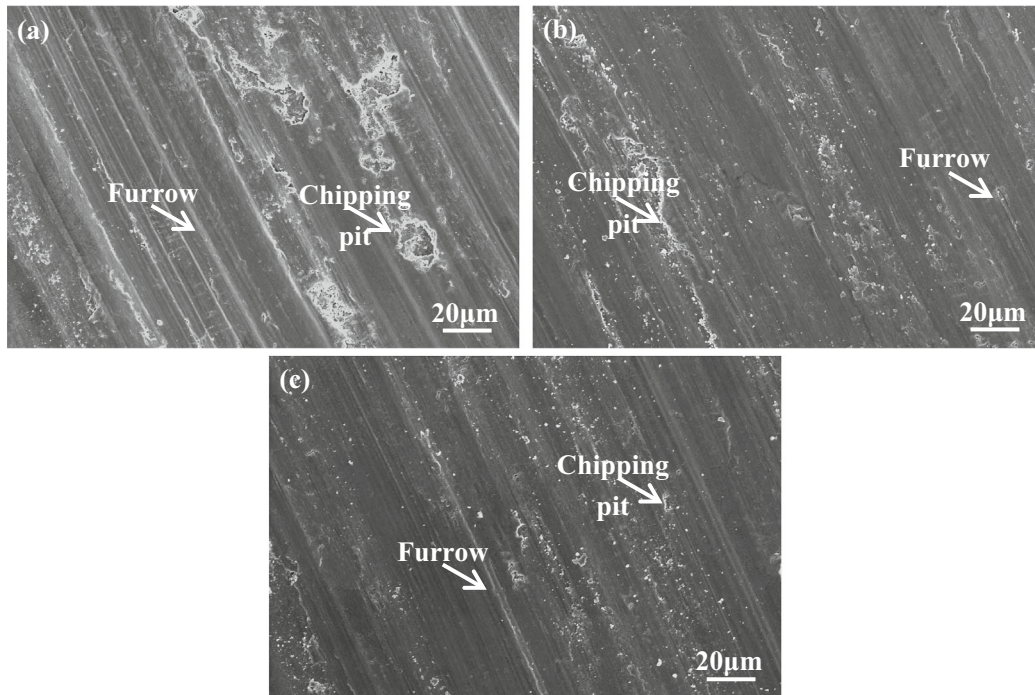


Figure 13. Wear surface morphology of Al-Si-Cu-Mg alloys under different casting processes.

Among the three casting processes, the alloys formed by semisolid squeeze casting have the best mechanical properties; tensile strength, elongation and Brinell hardness reach 187.67 MPa, 2.33% and 142.5 HB, respectively. Compared with gravity casting, they are increased by 55.07, 56.38 and 29.66%, respectively, due to the decrease in coarse primary Si particles, the increase in solute elements and higher dislocation density in the microstructure.

Owing to the uniform distribution of Si phases and equiaxed crystallization of α -Al phase in semisolid squeeze casting Al-Si-Cu-Mg alloys, the wear surface furrow is shallower and spalling pits are fewer.

Acknowledgements

The author expresses their gratitude to National Natural Science Foundation of China (No.51674168); Key-Area Research and Development Program of Guangdong Province (No.2020B010186002)

REFERENCES

1. V.A. Aranda, I.A. Figueroa, G. Gonzalez et al., Study of the microstructure and mechanical properties of Al-Si-Fe with additions of chromium by suction casting. *J. Alloy. Compd.* **853**, 1–9 (2021). <https://doi.org/10.1016/j.jallcom.2020.157155>
2. A.K. Dahle, K. Nogita, S.D. McDonald et al., Eutectic modification and microstructure development in Al-Si alloys. *Mater. Sci. Eng. A.* **413–414**, 243–248 (2005). <https://doi.org/10.1016/j.msea.2005.09.055>
3. Y. Nemri, B. Gueddouar, M.E.A. Benamar et al., Effect of Mg and Zn contents on the microstructures and mechanical properties of Al-Si-Cu-Mg alloys. *Int. Met.* **12**, 20–27 (2018). <https://doi.org/10.1007/s40962-017-0134-y>
4. M. Qi, Y. Kang, Q. Qiu et al., Microstructures, mechanical properties, and corrosion behavior of novel high-thermal-conductivity hypoeutectic Al-Si alloys prepared by rheological high-pressure die-casting. *J. Alloy. Compd.* **749**, 487–502 (2018). <https://doi.org/10.1016/j.jallcom.2018.03.178>
5. J. Hernandez-Sandoval, A.M. Samuel, F.H. Samuel et al., Effect of additions of SiC and Al₂O₃ particulates on the microstructure and tensile properties of Al-Si-Cu-Mg cast alloys. *Int. Met.* **10**, 253–263 (2016)
6. S.S. Wu, G. Zhong, P. An et al., Microstructural characteristics of Al-20Si-2Cu-0.4Mg-1Ni alloy formed by rheo-squeeze casting after ultrasonic vibration treatment. *Trans. Nonferrous. Met.* **12**, 2863–2870 (2012). [https://doi.org/10.1016/S1003-6326\(11\)61543-4](https://doi.org/10.1016/S1003-6326(11)61543-4)
7. H. Liu, L. Li, J. Niu et al., Effect of Mg and Cu additions on microstructure and mechanical properties of squeeze casting Al-Si-Cu-Mg alloy. *Mater. Sci. Forum.* **850**, 511–518 (2016). <https://doi.org/10.4028/www.scientific.net/MSF.850.511>
8. Y.L. Liu, C.J. Wu, H. Tu et al., Microstructure and mechanical properties of Al-10Si alloy modified with Al-5Ti. *China. Foundry.* **15**, 405–410 (2018)

9. M. Shafizadeh, H. Aashuri, S. Nikzad et al., Mechanical properties of Al-30Si-5Fe alloy using combination of rapid solidification and thixocasting processes. *Metallogr Microstruct Anal* **6**, 502–511 (2017). <https://doi.org/10.1007/s13632-017-0388-z>
10. H.M. Lus, Effect of casting parameters on the microstructure and mechanical properties of squeeze cast A380 aluminum die cast alloy. *Metal. Mater.* **4**, 270–277 (2012). https://doi.org/10.4149/km_2012_4_243
11. A. Maleki, A. Shafyei, B. Niroumand, Effects of squeeze casting parameters on the microstructure of LM13 alloy. *J. Mater. Process. Tech.* **8**, 3790–3797 (2009). <https://doi.org/10.1016/j.jmatprotec.2008.08.035>
12. C. Lin, S. Wu, S. Lue et al., Effects of high pressure rheo-squeeze casting on Fe-containing intermetallic compounds and mechanical properties of Al-17Si-2Fe-(0, 0.8) V alloys. *Mater. Sci. Eng. A.* **713**, 105–111 (2017). <https://doi.org/10.1016/j.msea.2017.12.050>
13. D. Vanluu, D.Z. Sheng, J.L. Wen, Effect of process parameters on microstructure and mechanical properties in AlSi9Mg connecting-rod fabricated by semi-solid squeeze casting. *Mater. Sci. Eng. A.* **558**, 95–102 (2012). <https://doi.org/10.1016/j.msea.2012.07.084>
14. A. Hekmat-Ardakan, X. Liu, F. Ajersch et al., Wear behaviour of hypereutectic Al-Si-Cu-Mg casting alloys with variable Mg contents. *Wear* **9**, 684–692 (2010). <https://doi.org/10.1016/j.wear.2010.07.007>
15. L. Lasa, J.M. Rodriguez-Ibabe, Wear behaviour of eutectic and hypereutectic Al-Si-Cu-Mg casting alloys tested against a composite brake pad. *Mater. Sci. Eng. A.* **1–2**, 193–202 (2003). [https://doi.org/10.1016/S0921-5093\(03\)00633-6](https://doi.org/10.1016/S0921-5093(03)00633-6)
16. K. Pratheesh, A. Kanjirathinkal, M.A. Joseph et al., Study on the effects of squeeze pressure on mechanical properties and wear characteristics of near-eutectic Al-Si-Cu-Mg-Ni piston alloy with variable Cu content. *Int. Met.* **11**, 831–842 (2017). <https://doi.org/10.1007/s40962-017-0132-0>
17. B.Z. Yan, M.L. Chang, W. Kai, The structural evolutions of ZL109 alloy and 7050 alloy in the semisolid squeeze casting process. *J. Wuhan. Univ. Technol.* **1**, 118–122 (2010). <https://doi.org/10.1007/s11595-010-1118-4>
18. K. Sukumaran, B.C. Pai, M. Chakraborty, The effect of isothermal mechanical stirring on an Al-Si alloy in the semisolid condition. *Mater. Sci. Eng. A.* **1–2**, 275–283 (2004). <https://doi.org/10.1016/j.msea.2003.11.036>
19. W. Dai, S. Wu, S. Lue et al., Effects of rheo-squeeze casting parameters on microstructure and mechanical properties of AlCuMnTi alloy. *Mater. Sci. Eng. A.* **538**, 320–326 (2012). <https://doi.org/10.1016/j.msea.2012.01.051>
20. L.L. Shu, S.W. Shu, W. Li et al., Microstructure and tensile properties of wrought Al alloy 5052 produced by rheo-squeeze casting. *Met. Mater. Trans. A.* **44**, 2735–2745 (2013)
21. S. Li, A. Zhao, W. Mao et al., Study on forming mechanism of sphere-like α phase in microstructure of semisolid hypereutectic Al-Si alloy. *Acta. Met.* **5**, 545–549 (2000)
22. Y. Zhang, X.P. Li, S.P. Sun et al., Microstructure evolution and mechanical properties of rheo-squeeze casting AZ91-Ca alloy during heat treatment. *China Foundry.* **6**, 485–491 (2017). <https://doi.org/10.1007/s41230-017-7025-y>
23. M.S. Salleh, M.Z. Omar, Influence of Cu content on microstructure and mechanical properties of thixo-formed Al-Si-Cu-Mg alloys. *Trans. Nonferrous Metal.* **11**, 352–353 (2015). [https://doi.org/10.1016/S1003-6326\(15\)63995-4](https://doi.org/10.1016/S1003-6326(15)63995-4)
24. S.G. Shabestari, E. Parshizfard, Effect of semi-solid forming on the microstructure and mechanical properties of the iron containing Al-Si alloys. *J. Alloys. Compd.* **509**, 7973–7978 (2011). <https://doi.org/10.1016/j.jallcom.2011.05.052>
25. I. Outmani, J. Isselin et al., Effect of Si, Cu and processing parameters on Al-Si-Cu HPDC castings. *J. Mater. Process. Tech.* **249**, 559–569 (2017). <https://doi.org/10.1016/j.jmatprotec.2017.06.043>
26. Y.D. Jia, Z.J. Wei et al., Effect of high-pressure solidification on tensile properties and strengthening mechanisms of Al-20Si. *J. Alloy. Compd.* **688**, 88–93 (2016). <https://doi.org/10.1016/j.jallcom.2016.07.016>
27. M. Akbari, M.H. Shojaeefard et al., Wear and mechanical properties of surface hybrid metal matrix composites on Al-Si aluminum alloys fabricated by friction stir processing. *Proc. Inst. Mech. Eng. Part L. J. Mater. Des. Appl* **223**(5), 790–799 (2017). <https://doi.org/10.1177/1464420717702413>
28. M. Qi, Y. Kang, Y. Xu et al., A novel rheological high pressure die-casting process for preparing large thin-walled Al-Si-Fe-Mg-Sr alloy with high heat conductivity, high plasticity and medium strength. *Mater. Sci. Eng. A.* **776**, 1–18 (2020). <https://doi.org/10.1016/j.msea.2020.139040>
29. X. Dong, X. Zhu, S. Ji, Effect of super vacuum assisted high pressure die casting on the repeatability of mechanical properties of Al-Si-Mg-Mn die-cast alloys. *J. Mater. Process. Tech.* **266**, 105–113 (2019). <https://doi.org/10.1016/j.jmatprotec.2018.10.030>
30. O. Prach, O. Trudonoshyn, P. Ranzelzhofer et al., Effect of Zr, Cr and Sc on the Al-Mg-Si-Mn high-pressure die casting alloys[J]. *Mater. Sci. Eng. A.* **759**, 603–612 (2019). <https://doi.org/10.1016/j.msea.2019.05.038>
31. S. Beroual, Z. Boumerzoug, P. Paillard et al., Comparative study on the microstructures and hardness of the AlSi10.6CuMg alloy produced by sand casting and high pressure die casting. *Int. Met.* **32**(4), 191–212

- (2019). <https://doi.org/10.1080/13640461.2019.1603681>
32. J.F. Archard, Contact and rubbing of flat surfaces. *J. Appl. Phys.* **24**(8), 981–988 (1953). <https://doi.org/10.1063/1.1721448>
33. M.I.A. El Aal, H.S. Kim, Wear properties of high-pressure torsion processed ultrafine grained Al-7%Si alloy[J]. *Mater. Des.* **53**, 373–382 (2014). <https://doi.org/10.1016/j.matdes.2013.07.045>
34. O. Zak, B. Tonn, A. Baesgen et al., New wear resistant hypereutectic AlSi₄Cu₄FeCrMn alloys for high pressure die casting. *Int. Met.* **9**, 49–57 (2015). <https://doi.org/10.1007/BF03356040>

Publisher's Note Springer Nature remains neutral with regard to jurisdictional claims in published maps and institutional affiliations.